Four-Electron Shell Structures and an Interacting Two-Electron System in Carbon-Nanotube Quantum Dots

S. Moriyama,[1,2] T. Fuse,[1,2] M. Suzuki,[1,3] Y. Aoyagi,[2] and K. Ishibashi[1,3,*]

[1]*Advanced Device Laboratory, The Institute of Physical and Chemical Research (RIKEN), 2-1, Hirosawa, Wako, Saitama 351-0198, Japan*

[2]*Interdisciplinary Graduate School of Science & Engineering, Tokyo Institute of Technology, 4259, Nagatsuta-cho, Midori-ku, Yokohama 226-8503, Japan*

[3]*CREST, Japan Science and Technology (JST), Kawaguchi, Saitama 332-0012, Japan*

(Received 1 August 2004; published 11 May 2005)

Low-temperature transport measurements have been carried out on single-wall carbon-nanotube quantum dots in a weakly coupled regime in magnetic fields. Four-electron shell filling was observed, and the magnetic field evolution of each Coulomb peak was investigated. Excitation spectroscopy measurements have revealed Zeeman splitting of single particle states for one electron in the shell, and demonstrated singlet and triplet states with direct observation of the exchange splitting at zero-magnetic field for two electrons in the shell, the simplest example of Hund's rule.

DOI: 10.1103/PhysRevLett.94.186806 PACS numbers: 73.22.−f, 73.23.Hk, 73.63.Fg

Because of recent developments in the growth techniques of high quality single-wall carbon nanotubes (SWNTs), individual SWNTs displaying quantum dot (QD) behavior have been produced. It is possible that this behavior is clearer than that in the semiconductor QDs [1], in terms of the analogy with natural atoms. Although the experiments on nanotube quantum dots reported so far have revealed various interesting physics, such as shell filling [2], Zeeman splitting [3], Kondo effect [4], and the electron-hole symmetry for a semiconducting SWNT QD [5], they have been observed in various systems with different coupling regimes and different nanotube types, i.e., SWNTs [2–7] and multiwall nanotubes (MWNTs) [8]. In this respect, the physics of nanotube quantum dots does not appear to be systematically understood.

One of the unique features of SWNT QDs is the large zero-dimensional (0D) energy spacing (Δ) [9], compared with the on-site Coulomb interaction energy (δU) and the exchange interaction energy (J). Besides, Δ can be as large as the single electron charging energy ($E_C = e^2/C_\Sigma$:C_Σ is the self-capacitance of the dot). These facts make it possible to observe shell structures, even though a number of electrons are contained in the dot. Another unique feature is the magnetic field (B-field) effect on the single particle state in SWNT QDs, where the Zeeman effect is the only important effect because of the small diameter of SWNTs. These features are in striking contrast to those of standard GaAs/AlGaAs two-dimensional electron gas (2DEG) QDs of submicron size, where the 0D levels are very likely to be mixed by electron-electron interactions, so that the shell structure can be observed only in a few electron QDs [10,11], and not in many-electron QDs [1]. The orbital effect of the B field on 2DEG QD cannot be ignored, which also makes the shell structures much more complicated [12].

In our experiment, we show that the SWNT QD is suitable for investigating the analogy of the QD with natural atoms, by presenting systematic low-temperature transport data in magnetic field. The two- and four-electron periodicities have been observed in Coulomb diamonds, but, here, we focus on the latter regime. The excitation spectroscopy revealed the simple Zeeman splitting of single particle states for one electron in the shell. The highlight of this Letter is that we have observed an artificial He atomlike behavior for two electrons in the shell, where the textbook model of the interacting two-electron system can be directly applied with observable single and triplet states that have an exchange energy difference at zero-magnetic field, the simplest example of Hund's rule.

A single quantum dot is easily formed in an individual SWNT, just by depositing metallic contacts on it, which in our case are Ti [Fig. 1(c)] [13]. In our fabrication process, a whole nanotube between the two contacts is likely to form a single quantum dot [14]. The resistance at room temperature was 220 kΩ, and did not change as the gate voltage was changed, suggesting that the measured nanotube was metallic. All measurements were carried out in a dilution refrigerator at a base temperature of $T_{\mathrm{mix}} =$ 40 mK [15]. A magnetic field (B) of up to 8 T was applied perpendicular to the tube axis. Figure 1 shows the Coulomb diamonds with a four-electron periodicity (a), as well as the addition energy with the same periodicity (b), both of which are understood by the four-electron shell model based on the twofold band degeneracy (A and B) in addition to the twofold spin degeneracy [17].

The magnetic field evolution of each Coulomb peak in one period is shown in Fig. 2(a), where the current magnitude is also indicated by the gray scale. The B field can be divided into three ranges, depending on the shell filling scheme. In the low B-field (I) region, each peak shifts linearly in alternate directions, indicating that electrons

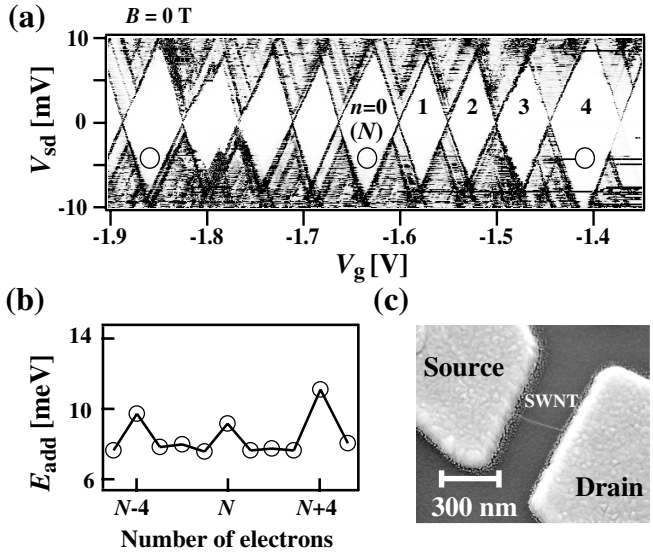

FIG. 1. (a) Gray scale plot of the differential conductance, dI_d/dV_{sd}, as a function of V_{sd} and V_g at $B = 0$ T. The number, n, indicates the number of electrons in a shell that can accommodate four electrons. The shell from $n = 0$ to 4 is investigated in details in this Letter. N is the number of total electrons in the dot. (b) Additional energy (E_{add}) as a function of N, determined by the size of the Coulomb diamonds in Fig. 1(a). (c) Scanning electron micrograph of the sample. The distance between the contacts was 300 nm.

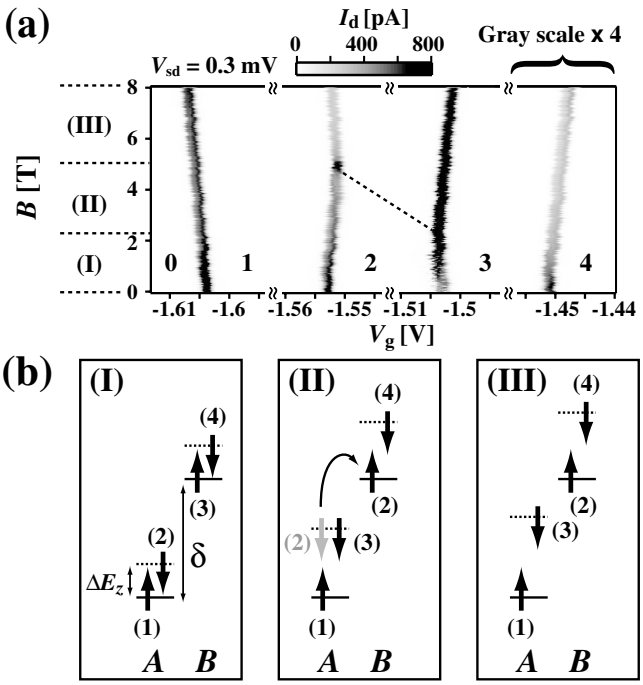

FIG. 2. (a) Magnetic field evolution of Coulomb peaks up to 8 T in the numbered range in Fig. 1(a). $V_{sd} = 0.3$ mV. The magnetic field range is divided into three parts, depending on the shell filling scheme. (b) Shell filling scheme estimated from the direction of the peak evolution in the three different magnetic field ranges. Single particle states are Zeeman splitted double states with opposite spins. ΔE_z corresponds to the Zeeman energy. Each number indicates (1) first, (2) second, (3) third, and (4) fourth electrons which come successively into the shell [25]. Note that the ''internal spin flip'' occurs in this range.

occupy successive levels from the lowest level, so that the total spin changes between 0 and $1/2$ as n is increased, producing an even-odd effect [18]. However, in the high B-field (III) region, two peaks move in together in the same direction, suggesting spin polarization. In this case, the total spin changes from $0 \rightarrow 1/2 \rightarrow 1 \rightarrow 1/2 \rightarrow 0$ as n increases. The intermediate B-field region (II) is between the two kinks that appear in the two lines in the middle. The different kink positions in the two lines suggest that an ''internal spin flip'' occurs during the gate sweep, as modeled in Fig. 2(b). At lower gate voltages, the second electron occupies the $A\downarrow$ state; however, as the gate voltage becomes larger, it flips to the $B\uparrow$ state, so that the third electron can occupy the $A\downarrow$ state. This effect may occur when the energy mismatch (δ) between the A and B states has a V_g dependence [6], so that the relative distance between the $A\downarrow$ and $B\uparrow$ states gets closer as V_g is swept.

The magnetic field evolution of the excited states as well as the ground state can be directly observed in the excitation spectroscopy measurements, as shown in Fig. 3(a) for the first ($n = 0 \leftrightarrow 1$) and second ($n = 1 \leftrightarrow 2$) stripes obtained from the Coulomb peaks with large V_{sd}. In the figure, dI_d/dV_g is plotted on a color scale as a function of V_g and B. A number of electrons are contained in the dot; however, we can focus only on a single shell composed of four states with similar energies, because the other shells are closed and separated by the large Δ.

The basic idea of the excitation spectroscopy is as follows. Suppose the gate voltage is swept such that the number of electrons in the dot is increased one by one. The current increases whenever a new state comes into the transport window set by V_{sd} because the number of transport channels increases. Once the current has increased to some certain value, it drops to zero (Coulomb blockade) when the first state that already exists in the transport window comes out of it, resulting in an increment of one electron in the dot [19]. The red lines indicate positive values, which is an indication of a new state coming into the transport window [20]. The blue line, which is negative, indicates the sudden drop of the current to zero due to the Coulomb blockade.

In the first stripe, the simple B-field evolution of each state is observed as lines indicated by A–D. Each line corresponds to Zeeman levels with up and down spins that successively come into the transport window [Fig. 3(b)]. The B-field dependence of the Zeeman splitting, lines A and B, for example, gives a g factor of 1.99 ± 0.07, a value similar to that of graphite and a value reported previously [3,6,21].

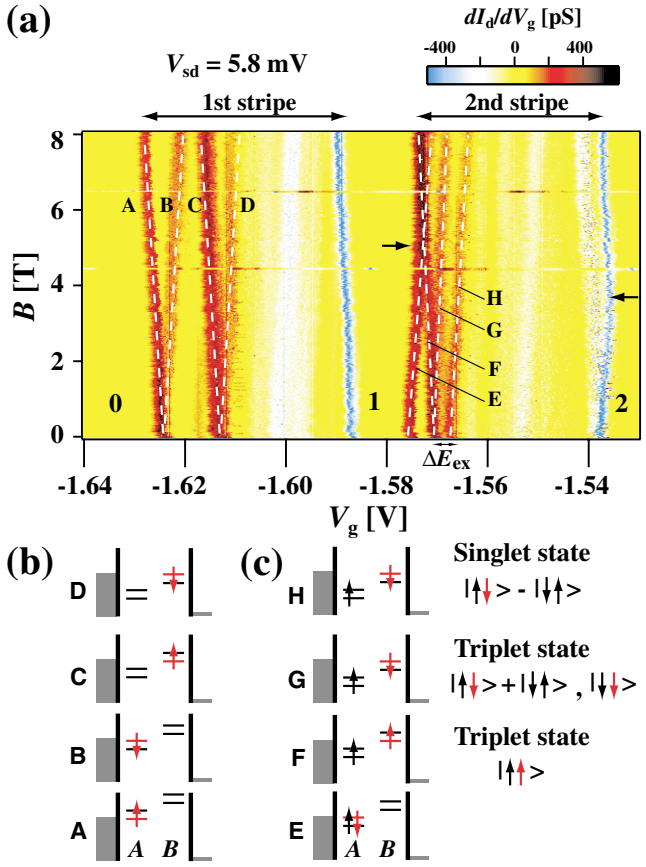

FIG. 3 (color). (a) Excitation spectroscopy measurements in the one- and two-electron systems in a magnetic field in the four-electron shell filling regime. dI_d/dV_g is calculated from I_d-V_g data with $V_{sd} = 5.8$ mV, and is plotted on a color scale as a function of V_g and B. Each line from A to H is due to a state shown by the energy diagrams in (b) for the one-electron system and (c) for the two-electron system.

The second stripe is more interesting in terms of the direct investigation of the interacting two-electron system. An extra electron is already contained in the dot before the new state comes into the transport window. Each of the experimentally observed red lines corresponds to a measurement of the state which is about to come into the transport window. Equivalently, the measurement corresponds to a projection of the state. The basic model is shown in Fig. 3(c). Line F is due to one of the triplet states ($|\uparrow\uparrow\rangle$). (The notation $|\uparrow\downarrow\rangle$, for example, indicates an up spin in the A subband and a down spin in the B subband). The $|\uparrow\downarrow\rangle + |\downarrow\uparrow\rangle$ and $|\downarrow\downarrow\rangle$ states are not possible in this case, because they have higher energy than the $|\uparrow\uparrow\rangle$ state in a B field. Line G occurs due to the triplet states, expressed by $|\uparrow\downarrow\rangle + |\downarrow\uparrow\rangle$ or $|\downarrow\downarrow\rangle$, which are now energetically possible after a slight increase of V_g from the situation for line F [22]. Of the superposition states, $|\uparrow\downarrow\rangle$ is always detected because the $B\downarrow$ state is used for the measurement. The $|\uparrow\downarrow\rangle + |\downarrow\uparrow\rangle$ and $|\downarrow\downarrow\rangle$ states, which should have a different energy in the B field, are not able to be distinguished in the present measurement scheme where the onset level or projected state also shifts as a function of the B field. Two states of the triplet are now available for current flow (line G), as compared with one state available for line F. Lines F and G meet when the B-field value goes to zero, which indicates degeneracy of the triplet state ($|\uparrow\uparrow\rangle$, $|\uparrow\downarrow\rangle + |\downarrow\uparrow\rangle$, and $|\downarrow\downarrow\rangle$) at $B = 0$ T. One might think three lines should be observed, associated with the triplet state. However, because of the above-mentioned measurement scheme, two lines can be observed. Line H, which runs just next to line G, is attributed to the singlet state, $|\uparrow\downarrow\rangle - |\downarrow\uparrow\rangle$, with a finite energy larger than the energy of the triplet state. The separation (ΔE_{ex}) between lines F and H at $B = 0$ T directly corresponds to the energy difference between the singlet and triplet states, the exchange energy J. This is a direct demonstration of the simplest example of the Hund's rule, in the sense that the higher spin state, $S = 1$ in the present case, is likely to occur due to the exchange effect which lowers the total energy.

We may also show the excitation spectroscopy data for the three- and four-electron shell filling regimes. However, the overall signals are rather small, and need further investigation for a full understanding of the effects.

It should be noted that the lines E and F cross in the second stripe, as indicated by the arrow, while crossing is not observed in the first stripe. The line crossing observed in the second stripe is closely related to the kink observed in the blue line, since the blue line should be a replica of the leftmost red line. The blue lines occur when the state that has first come into the transport window comes out of it, and the system is Coulomb blockaded. In fact, the expected behavior is shown in both the leftmost red and blue lines except for the different kink positions. This effect, indicated by the arrows, is again explained by the V_g dependent δ, as is the case in Fig. 2(a). Actually the slope of the line connected by the two arrows is consistent with that of the dotted line in Fig. 2(a).

Having understood the qualitative behavior of shell filling and the two-electron interaction behavior in the SWNT QD, we now estimate various energy scales associated with the dot. The addition energies for each Coulomb diamond that shows the four-electron periodicity contain information on interaction energies as well as the single particle level spacing [24]. Based on the Hamiltonian given in Ref. [24], the energy values are obtained as $\delta = 1.7 - 0.006\Delta V_g$ meV, $\Delta = 5.9$ meV, $E_C = 6.7$ meV, $\delta U = 0.4$ meV, and $J = 0.5$ meV. ΔV_g is measured from the first Coulomb peak position ($n = 0 \leftrightarrow 1$) at $B = 0$. J and δ at $\Delta V_g = 0$ were obtained directly from the exchange splitting (ΔE_{ex}) in Fig. 3(a) and the first excited line in the Coulomb diamond of Fig. 1(a), respectively. The condition, $\delta < \Delta/2$, necessary for observation of the four-electron periodicity, is, in fact, satisfied. The estimated energy values are consistent with the "internal spin flip"

condition, $J + \delta U = \delta - \Delta E_z$ [25], at the kink positions in Figs. 2(a) and 3(a). Δ as large as E_C is unique for SWNT QD. The simple theoretical estimate of Δ (= 5.6 meV), based on $h v_F/2L$ (L, the length of the contact gap, is 300 nm and is equivalent to the dot size, $v_F = 8.1 \times 10^5$ m/s) where subband degeneracy is assumed, is in good agreement with obtained Δ (= 5.9 meV) in the experiment. This fact indicates that the quantum levels indeed originate from the one-dimensional confinement of electrons in the tube-axis direction. The estimated energy parameters normalized by Δ appear to be consistent with the previously reported [7] and predicted [24] values, and confirm the unique condition in the SWNT QD, which is mentioned in the introductory part. It is interesting to note that the on-site Coulomb energy and the exchange interaction energies are three or four orders smaller in the SWNT QD than those values of the natural He atom [26], which might be reasonable because of the large difference in the space where electrons are confined.

In summary, we have carried out low-temperature transport measurements in individual SWNT QDs. The four-electron shell filling regime has been carefully investigated, and the magnetic field evolution of each Coulomb peak has revealed the different shell fillings in low, high, and intermediate magnetic field ranges. Excitation spectroscopy measurements have been carried out in the one- and two-electron regimes, and the interacting two-electron model in a magnetic field was directly observed.

We thank Professor M. Eto of Keio University for useful discussions and suggestions. We also enjoyed discussions with Dr. A. Furusaki and Dr. Y. Ishiwata of RIKEN.

*Electronic address: kishiba@riken.jp

[1] L. P. Kouwenhoven, *et al.*, in *Mesoscopic Electron Transport*, NATO ASI, Ser. E, Vol. 345 (Kluwer Academic Publishers, Dordrecht, The Netherlands, 1997).
[2] D. H. Cobden *et al.*, Phys. Rev. Lett. **89**, 46803 (2002).
[3] D. H. Cobden *et al.*, Phys. Rev. Lett. **81**, 681 (1998).
[4] J. Nygård *et al.*, Nature (London) **408**, 342 (2000).
[5] P. Jarillo-Herrero *et al.*, Nature (London) **429**, 389 (2004).
[6] S. J. Tans *et al.*, Nature (London) **394**, 761 (1998).
[7] W. Liang *et al.*, Phys. Rev. Lett. **88**, 126801 (2002).
[8] M. R. Buitelaar *et al.*, Phys. Rev. Lett. **88**, 156801 (2002).
[9] Throughout this Letter, we distinguish the 0D energy spacing, Δ, and the subband mismatch, δ. Δ is determined by the one-dimensional confinement in the tube-axis direction and is the same for both subbands, while δ is determined by the mismatch between the two (A and B) subbands.
[10] S. Tarucha *et al.*, Phys. Rev. Lett. **77**, 3613 (1996).
[11] M. Ciorga *et al.*, Phys. Rev. Lett. **88**, 256804 (2002).
[12] L. P. Kouwenhoven *et al.*, Science **278**, 1788 (1997).
[13] M. Bockrath *et al.*, Science **275**, 1922 (1997).
[14] M. Suzuki *et al.*, J. Vac. Sci. Technol. B **19**, 2770 (2001).
[15] The effective temperature, $T_e = 240$ mK, was estimated by fitting the Coulomb peak measured at $V_{sd} = 10\ \mu$V with the quantum version of the theoretical expression of the peak [16].
[16] C. W. J. Beenakker, Phys. Rev. B **44**, 1646 (1991).
[17] R. Saito *et al.*, *Physical Properties of Carbon Nanotubes* (Imperial College Press, London, 1998).
[18] D. C. Ralph *et al.*, Phys. Rev. Lett. **78**, 4087 (1997).
[19] N. C. van der Vaart *et al.*, Physica (Amsterdam) **189B**, 99 (1993).
[20] Precisely speaking, it is likely that some of the states in the lower closed shell may also exist in the transport window when the Coulomb blockade is lifted, since the applied $V_{sd} = 5.8$ mV is very close to the estimated Δ. Some of the white lines, such as those which appear at $V_g \sim -1.6$ and -1.555 V in Fig. 3(a) are related to this fact. However, the effect of the lower closed shell on the electronic state of the open shell can be ignored.
[21] There appears to be a slight deviation from the straight line above $B = 4$ T for line D. This may be explained by considering that the magnetic field evolution of the onset of the new state coming into the transport window may be strongly affected by the magnetic field dependence of other already existing states.
[22] The $|\downarrow\downarrow\rangle$ is possible in such a case where the original $A\uparrow$ electron is replaced by a $A\downarrow$ electron before the $B\downarrow$ state comes into the transport window, because the spin blockade mechanism does not allow the $|\downarrow\downarrow\rangle$ configuration [23]. (The absolute change of S_z becomes more than $1/2$.)
[23] D. Weinmann *et al.*, Phys. Rev. Lett. **74**, 984 (1995).
[24] Y. Oreg *et al.*, Phys. Rev. Lett. **85**, 365 (2000).
[25] The additional energies, $E_{add}(n)$ of each region are as follows. For $J + \delta U < \delta - \Delta E_z$ (low magnetic field): $E_{add}(1) = \Delta + E_C - \delta U - \delta - \Delta E_z$, $E_{add}(2) = E_{add}(4) = E_C + \delta U + J + \Delta E_z$, $E_{add}(3) = E_C + \delta - \delta U - \Delta E_z$. For $J + \delta U > \delta - \Delta E_z$ (high magnetic field): $E_{add}(1) = \Delta + E_C - \delta U - \delta - \Delta E_z$, $E_{add}(2) = E_{add}(4) = E_C + \delta$, $E_{add}(3) = E_C + \delta U + 2J - \delta + \Delta E_z$. These equations are deduced by calculating the Hamiltonian of the nanotube quantum dot, given in Ref. [24].
[26] J. J. Sakurai, *Modern Quantum Mechanics* (The Benjamin/Cummings Publishing Company, Menlo Park, CA, 1985).